DISCRETE ELEMENT MODELING AND PARAMETER CALIBRATION FOR CORYDALIS TUBER
/
延胡索离散元模型构建及参数标定

Xiangyang LIU[1)], Chun WANG[1,2)], Yongchao SHAO[1)], Weiguo ZHANG[1*)]
[1)]College of Mechanical and Electrical Engineering, Northwest Agriculture and Forestry University, Yangling 712100, China;
[2)]College of Biological and Agricultural Engineering, Jilin University, Changchun 130000, China
Tel: +86-17391612856; E-mail: cn-lxy@nwafu.edu.cn
DOI: https://doi.org/10.35633/inmateh-76-02

Keywords: *Corydalis tuber, discrete element, parameter calibration, optimal design*

ABSTRACT
To address the lack of contact parameters between Corydalis tuber and mechanical, or soil interfaces during planting, harvesting, and processing stages, this study calibrated discrete element simulation parameters for Corydalis tuber by combination of simulation tests and physical tests. 3D contour model of Corydalis tuber was obtained using 3D scanning technology, and a multi-sphere bonded particle model was constructed by automatic filling method. Simulation tests were conducted with the restitution coefficient, static friction coefficient, and rolling friction coefficient between Corydalis tuber and Q235 steel, as well as between Corydalis tuber and soil, as independent variables. The rebound height, friction angle, and rolling distance were considered as dependent variables. A second-order polynomial fitting method was used to analyze the experimental results. The actual test values were substituted into the polynomial equations to obtain simulation values for the contact parameters of Corydalis tuber with Q235 steel and soil, and these values were then validated against the experimental results. The findings indicate that the restitution coefficients of Corydalis tuber-Q235 steel and Corydalis tuber-soil were 0.728 and 0.44, respectively. The static friction coefficients of Corydalis tuber-Q235 steel and Corydalis tuber-soil were 0.41 and 0.76, respectively, while the rolling friction coefficients were 0.02 and 0.033, respectively. Under these conditions, the relative error between the simulation tests and physical tests was minimized. This study provides calibrated particle models and contact parameters for mechanical processing applications, including sowing, harvesting, and drying of Corydalis tuber.

摘要
针对延胡索在种植、收获、加工等环节中缺乏与机械、土壤接触参数的现状，本研究结合仿真试验与物理试验对延胡索进行离散元仿真参数标定。借用三维扫描技术获得延胡索的三维轮廓模型，采用自动填充法建立延胡索的多球粘结颗粒模型。分别以延胡索与 Q235 钢、土壤的碰撞恢复系数，静摩擦因数及滚动摩擦因数为自变量，以碰撞高度、摩擦倾角及滚动距离为因变量进行仿真试验，并进行二次多项式拟合。将实际试验值带入二次多项式，获得延胡索与 Q235 钢、土壤的接触参数仿真值，并与实际试验值进行校对。试验结果表明：延胡索-Q235 钢，延胡索-土壤的碰撞恢复系数分别为 0.728、0.44；延胡索-Q235 钢，延胡索-土壤的静摩擦因数分别为 0.41、0.76；延胡索-Q235 钢，延胡索-土壤的碰撞恢复系数分别为 0.02、0.033 时，仿真试验与实际试验相对误差最小。本研究可为延胡索播种、收获及烘干等机械加工提供颗粒模型与仿真接触参数。

INTRODUCTION
Corydalis tuber is one of the most widely utilized medicinal herbs in China. It is characterized by a flattened, spherical shape and typically thrives in loose soils, such as sandy or semi-sandy environments. Corydalis tuber contains over 30 types of alkaloids, including tetrahydropalmatine and corydaline (*He et al., 2007; Chen et al., 2008*). It exhibits notable pharmacological effects, such as analgesic, sedative, hypnotic, and anti-arrhythmic properties. In recent years, with the expanding applications of Corydalis tuber in the medical field, its demand has continued to rise, leading to increased profitability in its cultivation. Hanzhong City in Shaanxi Province is the largest Corydalis tuber cultivation area in China, with over 100,000 acres under cultivation, accounting for more than 70% of the nation's total production. Currently, the cultivation and harvesting of Corydalis tuber rely predominantly on manual labor, resulting in high labor intensity and elevated costs, which severely constrain the development of its cultivation industry.

To achieve full mechanization across all stages of Corydalis tuber cultivation, from planting to harvesting, has become an urgent necessity. Objective and accurate collection of the mechanical property parameters of Corydalis tuber is a prerequisite for the development of specialized mechanized equipment (*Han et al., 2017; Liu et al., 2018; Ma et al., 2013; Shi et al., 2014*).

The DEM simulates granular materials discretely, modeling each particle independently and assigning it mass, stiffness, and damping properties. The particles interact with each other through contact, and the dynamic forces and moments at the contact points are calculated using a contact mechanics model (such as the Hertz-Mindlin model), which in turn predicts the motion state of individual particles. This method has unique advantages in studying the plant-soil interaction in mechanized farming: First, it breaks through the continuum assumption and directly characterizes the particle-level stress transfer and displacement processes in the microscopic contact between the agricultural tool and the soil, accurately analyzing the soil fragmentation/compaction mechanism. Second, its multi-physics coupling capability can simultaneously simulate the stress deformation of mechanical components and the dynamic response of the soil, providing a cross-scale analysis basis for the structural optimization of agricultural machinery. This discrete granular dynamics feature makes it an important tool for shortening the research and development cycle of agricultural machinery.

Originally developed to solve geotechnical problems, the discrete element method (DEM) is a numerical method for calculating the mechanical properties of granular materials. It simulates granular materials as individual particles and calculates the forces (such as contact and friction forces) and movements between the particles iteratively over time steps. It is particularly suitable for studying plant-soil interactions in mechanized farming because it can capture the discrete nature of soil particles and irregular shapes of crops (e.g., tubers), enabling precise modeling of dynamic processes such as soil penetration, root-soil adhesion, and mechanical harvesting collisions (*Wang et al., 2024*). In agricultural research, DEM has been widely applied to model interactions between crops (e.g., seeds, roots) and soil or machinery. For example, DEM has been successfully used to optimize soil-tool interactions in potato harvesting by simulating tuber-soil separation processes. (*Zhao et al., 2023*), and to design seed metering devices by analyzing seed motion under dynamic conditions. As a result, the potato tubers obtained by DEM simulation analysis are more stable, and the leakage rate and replay rate (coefficient of variation) are lower under reasonable seeding device structure design and working parameters (forward speed of machine, seeding speed, etc.) (*Chen et al., 2023*). Xu Bing et al., (*2021*) developed a discrete element model for buckwheat seeds using an automatic filling method, followed by parameter calibration. Based on this model, they conducted an optimized design of the three-stage vibration process for buckwheat. The optimized three-stage vibrating screen has higher clearance rate and lower impurity rate. Chen Zeren et al., (*2018*) classified corn seeds by shape and developed discrete element models for corn seeds using varying numbers of spheres in a filling method. This approach aimed to balance computational efficiency and accuracy. The results were validated through a "self-flow screening" experiment, demonstrating close alignment with actual outcomes. Recent studies on root crop mechanization (e.g., sugar beet harvesting) have further validated DEM's accuracy in predicting tuber damage rates under varying soil conditions (*Yang et al., 2023*). These applications demonstrate DEM's capability to capture granular behavior and complex mechanical interactions, which is critical for analyzing Corydalis tuber in soil environments. For example, analyze the uniformity and stability of Corydalis tubers seeding, harvest rate at harvest, loss rate, etc.

Due to the flattened, irregular shape of Corydalis tuber and its dynamic interactions with soil during mechanized harvesting, the discrete element method (DEM) is a preferred approach to capture these complex behaviors. Addressing the lack of particle contact parameters essential for designing key machinery for sowing and harvesting Corydalis tuber, this study employed 3D scanning technology to obtain a three-dimensional model of Corydalis tuber. Using an automatic filling method, a discrete element model for Corydalis tuber was established (*Sun et al., 2022; Wang et al., 2017; Xu et al., 2022; Yu et al., 2020; Xu et al., 2018*). Simulation experiments were conducted with this model to determine the coefficients of restitution, static friction, and rolling friction between Corydalis tuber and both soil and Q235 steel. These simulations were then compared with actual tests to obtain mechanical parameters closest to the true values.

MATERIALS AND METHODS

Determination of fundamental physical parameters

The experimental subject selected was Corydalis tuber, harvested in early May from a designated experimental field in Chenggu County, Hanzhong City, Shaanxi Province, China, cultivated with the "Zhehu

No.1" variety. Sampling was conducted using the five-point sampling method, and subsequent measurements of its physical characteristic parameters were performed. The density of Corydalis tuber was measured using the water displacement method, yielding a density of 1085 kg/m³. The moisture content of Corydalis tuber at harvest was determined using an Ohaus M23 rapid moisture analyzer. The average moisture content obtained was 61.27%.

Determination of contact parameters

During the harvest period, interactions occur between the Corydalis tuber, as well as between the particles and the soil or machinery. In discrete element simulations, the restitution coefficient, static friction coefficient, and rolling friction coefficient play crucial roles in determining the accuracy and reliability of the simulation. The soil selected for the experiment was that typically used for cultivating Corydalis tuber in the local region, while the material chosen for the machinery components was Q235 steel.

Determination of the restitution coefficients of Corydalis tuber - Q235 steel, Corydalis tuber - soil

The restitution coefficient refers to the ratio of the separation velocity to the approach velocity in the normal direction at the point of contact before and after a collision, depending solely on the materials involved. The restitution coefficients for Corydalis tuber colliding with Q235 steel and soil were determined through a free-fall test, as depicted in Figure 1. Corydalis tuber was dropped from a height of 200 mm, and upon collision with the Q235 plate or soil bed, they bounced back. The rebound height *h* was recorded using a high-speed imaging system, with a scale-marked grid paper and steel ruler placed behind the particles. To ensure the reliability of the experimental data, 10 sets of tests were conducted, with each set repeated three times, and the average value was taken.

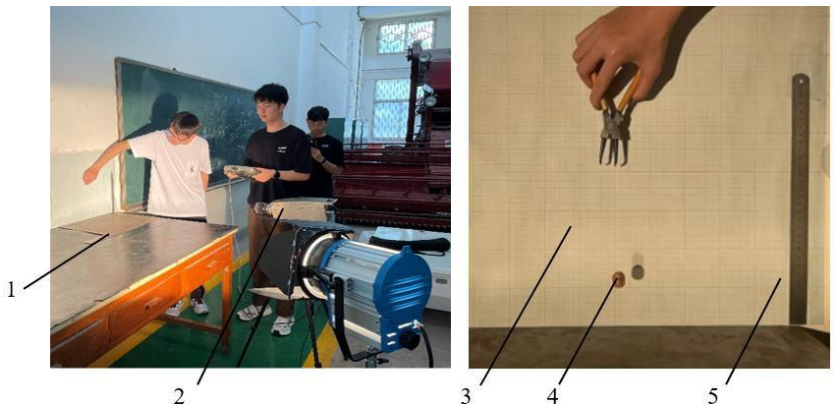

(a) Free fall test (b) Positive perspective of the free fall test

Fig. 1 - Determination of restitution coefficients of Corydalis tuber – Q235 steel, Corydalis tuber - soil

1. Q235 steel; 2. High-speed camera; 3. Graph paper; 4. Corydalis tuber; 5. Ruler.

The coefficient of restitution can be calculated using the following formula:

$$e = \frac{v_4 - v_3}{v_2 - v_1} \quad (1)$$

$$v_4 = \sqrt{2gh} \quad (2)$$

$$v_2 = \sqrt{2gH} \quad (3)$$

in which:

e – the coefficient of restitution between Corydalis tuber and the colliding material;

v_1 – the velocity of the colliding material before the collision, [m/s];

v_2 – the velocity of Corydalis tuber before the collision, [m/s];

v_3 – the velocity of the colliding material after the collision, [m/s];

v_4 – the velocity of Corydalis tuber after the collision, [m/s];

H – the height from which the object is dropped before free fall, [m];

h – the rebound height, [m];

g – the acceleration due to gravity, [m/s^2].

Both materials underwent 10 sets of experiments, and the results are presented in Table 1.

Table 1

Restitution coefficients of Corydalis tuber – Q235 steel, Corydalis tuber - soil

Number	Corydalis tuber-Q235 rebound height (m)	The coefficient of restitution	Corydalis tuber-soil rebound height (m)	The coefficient of restitution
1	0.0307	0.3916	0.0180	0.3000
2	0.0667	0.5774	0.0110	0.2345
3	0.0443	0.4708	0.0213	0.3266
4	0.0267	0.3651	0.0220	0.3317
5	0.0658	0.5730	0.0170	0.2915
6	0.0773	0.6218	0.0157	0.2799
7	0.0763	0.6178	0.0160	0.2828
8	0.0513	0.5066	0.0270	0.3674
9	0.0760	0.6164	0.0247	0.3512
10	0.0570	0.5339	0.0147	0.2708
The average value	**0.0572**	**0.5274**	**0.0187**	**0.3036**

By substituting the average rebound height of Corydalis tuber on Q235 steel and soil into Equation 2, 3 and 1, the coefficient of restitution of Corydalis tuber-Q235 is obtained as 0.5274, and the coefficient of restitution of Corydalis tuber-soil is 0.3036.

Determination of the static friction coefficients of Corydalis tuber - Q235 steel, Corydalis tuber - soil

The static friction coefficient refers to the ratio of the maximum static friction force to the normal force between two objects. The factors influencing the static friction coefficient mainly include the type of friction materials, the roughness of the contact surfaces, and so on. The static friction coefficients between Corydalis and Q235 steel, as well as between Corydalis and soil, were measured using the inclined plane method, as shown in Figures 2. Since Corydalis tuber have a flattened spherical shape, rolling is likely to occur during the experiment. To ensure accuracy and reduce experimental errors, four Corydalis tubers were bonded into a square shape using a hot glue gun. The inclined plane was equipped with an angle measurement device for easy reading and recording of data. For both materials, 10 sets of experiments were conducted, with each set repeated 3 times, and the average value was taken.

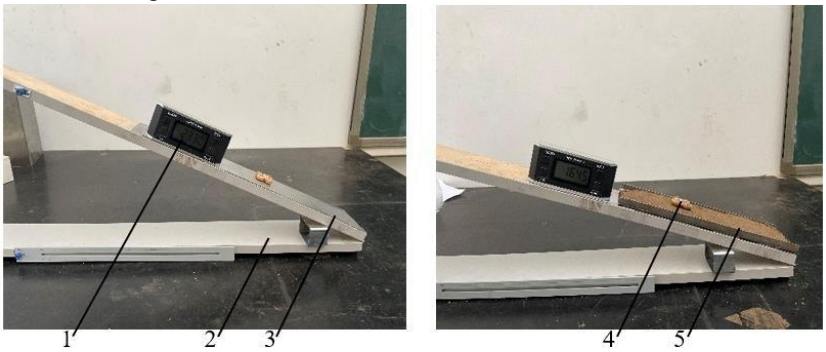

(a) Inclined plane method between Corydalis tuber and Q235 (b) Inclined plane method between Corydalis tuber and Soil

Fig. 2 - Determination of static friction coefficients of Corydalis tuber – Q235 steel, Corydalis tuber - soil

1. Angle measuring device; 2. Friction angle measuring instrument; 3. Q235 steel plate; 4. Corydalis tuber; 5. Soil plate.

The formula for calculating the static friction coefficient is as follows:

$$f = G\sin\theta \tag{4}$$

$$F_N = G\cos\theta \tag{5}$$

$$f = \mu F_N \tag{6}$$

in which: f – the frictional force acting on Corydalis tuber, [N];
G – the gravitational force of Corydalis tuber, [N];
F_N – the support force acting on Corydalis tuber, [N];
μ – the static friction coefficient;
θ – the angle between the inclined plane and the horizontal surface, [°].

Both materials underwent 10 sets of experiments, and the results are presented in Table 2.

Table 2

Static friction coefficients of Corydalis tuber – Q235 steel, Corydalis tuber - soil

Number	Corydalis tuber-Q235 static friction angle (°)	The static friction coefficient	Corydalis tuber-soil static friction angle (°)	The static friction coefficient
1	25.95	0.4867	38.88	0.8064
2	26.12	0.4903	38.88	0.8064
3	26.50	0.4986	41.18	0.8749
4	28.05	0.5328	40.18	0.8632
5	24.42	0.4540	40.97	0.8683
6	25.48	0.4766	39.43	0.8224
7	24.05	0.4463	42.38	0.9126
8	25.25	0.4716	38.83	0.8050
9	28.52	0.5433	40.77	0.8622
10	27.89	0.5292	42.12	0.9041
Average value	26.22	0.4925	40.43	0.8525

In the ten groups of tests of these two types of materials, the static friction angle between Corydalis tuber and Q235 ranges from 24.05° to 28.52°, and the static friction angle between Corydalis tuber and soil ranges from 38.83° to 42.38°. The surface roughness of the corresponding material plate (Q235 steel plate or soil plate) has been ensured to be continuously consistent before each Corydalis tuber test, and the surface condition of the particles of the Corydalis tuber used for test is unchanged. The friction angle measuring instrument used for the test had an accuracy of $\pm$ 0.2°, and the corresponding angle was displayed during the measurement (two decimal places were retained by default). The experimental environment and the accuracy of the measuring instrument complied with the specifications.

By substituting the average static friction angle of Corydalis tuber on Q235 steel and soil into Equation 4, 5 and 6, the static friction angle of Corydalis tuber-Q235 is obtained as 0.4925, and the static friction angle of Corydalis tuber-soil is 0.8525.

Determination of the rolling friction coefficients of Corydalis tuber – Q235 steel, Corydalis tuber - soil

Rolling friction occurs when an object rolls without slipping or tends to roll on another object's surface, causing deformation at the contact point between the two materials, which generates resistance to rolling. In this study, the rolling friction coefficient between Corydalis and Q235 steel plate, as well as between Corydalis and soil, was measured using the bevel rolling method. The experimental setup is shown in Figure 3.

In the rolling friction factor measurement, the Corydalis tuber roll without sliding on the inclined plane, and the rolling resistance generated by the steel plate on the Corydalis tuber is essentially static friction. According to the results measured in Table 2, the average static friction angle between the Corydalis tuber and Q235 is 26.22°. And in order to facilitate the fixation of the inclined plane and horizontal plate of the steel plate, the angle between the inclined plane and horizontal surface was set to 30°, ensuring the plane interface was as smooth as possible. Corydalis tuber was placed at a distance of L = 35 mm, and with an initial velocity of 0 m/s, they were allowed to roll freely until they stopped. The horizontal rolling distance (S) of the Corydalis tuber was measured. Ten sets of experiments were conducted for each material, with each set repeated three times. The average rolling distance was taken as the final data. The shape of the Corydalis tuber is mostly irregular and flattened spherical, and the size is relatively small and highly variable, air resistance cannot be ruled out during testing, so it may have a slight effect on the test results in actual measurement.

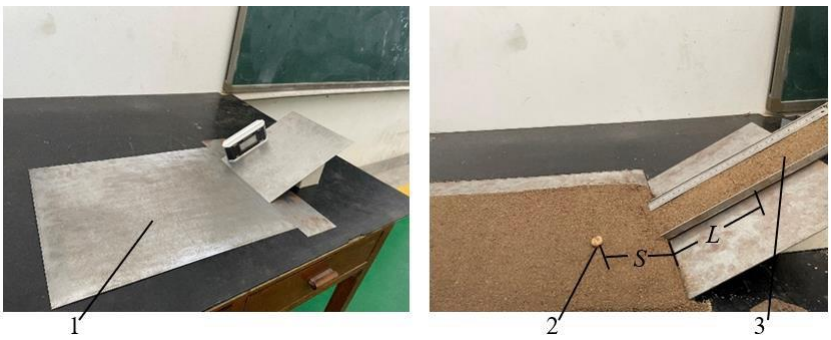

Fig. 3 - Determination of rolling friction coefficients of Corydalis tuber – Q235 steel, Corydalis tuber – soil
(a) Bevel rolling method between Corydalis tuber and Q235; (b) Bevel rolling method between Corydalis tuber and Soil
1. Q235 steel plate; 2. Corydalis tuber; 3. Soil plate.

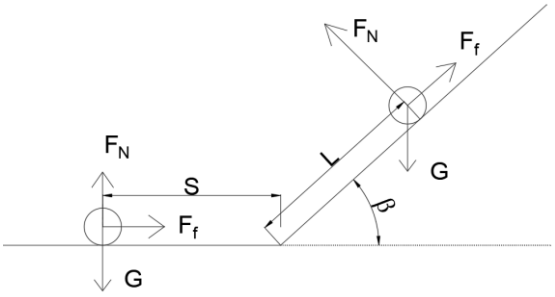

Fig. 4 - Force analysis of the Corydalis tuber rolling process

The force analysis of the rolling process of Corydalis tuber particles is shown in Figure 4. According to the law of conservation of energy during the entire rolling process, the rolling friction coefficient μ' can be calculated as follows:

$$0 - 0 = GL\sin\beta + (-\mu' G\cos\beta\, L) + (-\mu' GS)$$

$$GL\sin\beta = G(L\cos\beta + S)\mu'$$

$$\mu' = \frac{L\sin\beta}{L\cos\beta + S} \tag{7}$$

in which: β – the angle of inclination of the inclined plane, [°];

S – the distance traveled by Corydalis tuber while rolling on a flat surface, [m];

L – the distance traveled by Corydalis tuber while rolling on an inclined plane, [m];

μ' – the rolling friction coefficient of Corydalis tuber and materials.

Both materials underwent 10 sets of experiments, and the results are presented in Table 3.

Table 3

Rolling distances of Corydalis tuber – Q235 steel, Corydalis tuber - soil

Number	Corydalis tuber-Q235 rolling distance (mm)	Corydalis tuber-soil rolling distance (mm)
1	108.7	65.0
2	109.7	66.3
3	167.0	46.3
4	135.3	40.0
5	114.0	59.7
6	129.3	57.3
7	117.3	35.0
8	109.3	44.3
9	142.3	54.3
10	149.7	44.0
Average value	**122.1**	**49.7**

By substituting the average rolling distances of Corydalis tuber on Q235 steel and soil into Equation 7, the rolling friction coefficient of Corydalis tuber-Q235 is obtained as 0.115, and the rolling friction coefficient of Corydalis tuber-soil is 0.219.

Establishment of the Discrete Element Model for Corydalis tuber

3D model of Corydalis tuber

Given the highly irregular shape of Corydalis tuber, modeling using traditional three-dimensional software proves to be challenging (*Zhang et al., 2024*). In this study, advanced three-dimensional imaging technology was employed, utilizing the HandySCAN3D scanner to capture the three-dimensional morphology of Corydalis tuber (The surface roughness of the Corydalis tuber, deformation of the tuber and slight compression have negligible effects on the accuracy of the model.). The scanner has an accuracy of 0.0025 mm and a measuring rate of 1,300,000 measurements per second， then the contour model was saved in STL file format, as shown in Figure 5.

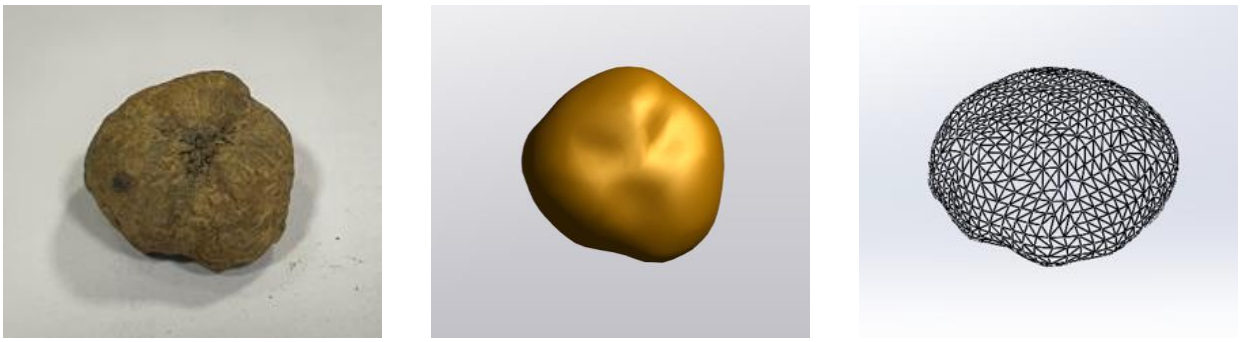

(a) Corydalis tuber (b) 3D model of Corydalis tuber (c) Corydalis tuber Outline model

Fig. 5 - The 3D model of Corydalis tuber

Discrete element model

In this study, a multi-sphere bonded particle model was employed to establish the discrete element model for Corydalis tuber. The previously scanned contour model of Corydalis tuber was used as the filling space. Spherical particles with diameters of 1 mm, 2 mm, and 4 mm were utilized for the filling, with the respective quantities of spherical particles being 3,439, 426, and 61, as shown in Figure 6. In consideration of both the accuracy of the equilibrium simulation and simulation speed, spherical particles with a diameter of 2 mm were ultimately selected for the particle filling of Corydalis tuber.

(a) 1mm (2) 2mm (3) 4mm

Fig. 6 - Multi ball bonding model

Calibration of contact parameters between Corydalis tuber, Q235 steel and soil

There exists a discrepancy between the parameters used in actual experiments and those in the simulations, making them unsuitable for direct application in subsequent mechanical simulation (*Zhao et al., 2024*). To enhance the accuracy and reliability of the discrete element simulations, calibration of the relevant parameters was performed through simulation experiments.

Calibration of the coefficient of restitution

Based on the coefficient of restitution of Corydalis tuber with Q235 steel and soil obtained from previous drop tests, the established discrete element model of Corydalis tuber was utilized to create simulation experiments under actual test conditions, as shown in Figure 7.

Fig. 7 - Drop test simulation

1. Corydalis tuber; 2. Baseplate.

In the simulation experiments, the static friction coefficient and rolling friction coefficient between the Corydalis tuber, Q235 steel, and soil were set to 0. Based on the results of the actual experiments, the coefficient of restitution for collisions between Corydalis tuber and Q235 was selected within the range of 0.3 to 0.8, while the coefficient of restitution for collisions between Corydalis tuber and soil was selected within the range of 0.05 to 0.65. The experimental results and the quadratic curve fitting results are shown in Figure 8.

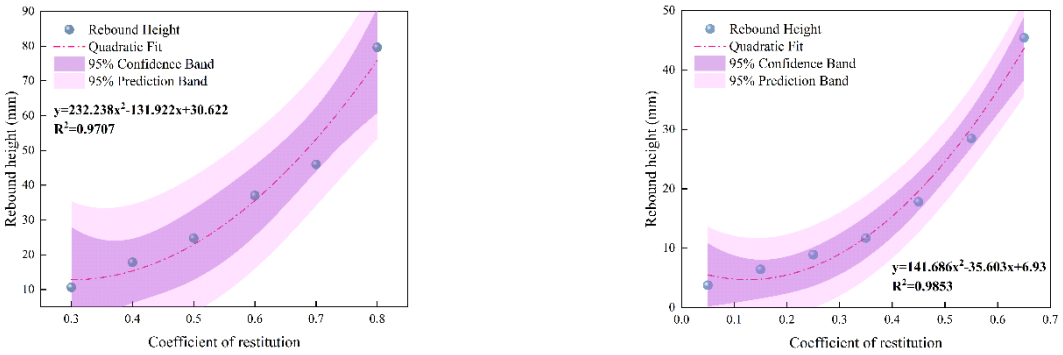

(a) Corydalis tuber - Q235 steel (b) Corydalis tuber - soil

Fig. 8 - The fitted curves of the coefficient of restitution and rebound height from impact simulation tests of Corydalis tuber with Q235 steel and soil

To establish the functional relationship between the coefficient of restitution and rebound height for collisions between Corydalis tuber and Q235 steel, as well as soil, a quadratic polynomial fitting was performed.

The equation of the fitting curve is as follows:

$$y_1 = 232.238x_1^2 - 131.922x_1 + 30.622 \quad (8)$$

$$y_2 = 141.686x_2^2 - 35.603x_2 + 6.93 \quad (9)$$

in which: y_1 – the rebound height of Corydalis tuber and Q235 steel, [m];

x_1 – the coefficient of restitution between Corydalis tuber and Q235 steel;

y_2 – the rebound height of Corydalis tuber and soil, [m];

x_2 – the coefficient of restitution between Corydalis tuber and soil.

The coefficient of determination for regression equation y_1 was R^2 = 0.9707, and for y_2, it was R^2 = 0.9853. Both models had P << 0.05, indicating that the regression models were highly significant. Substituting the average rebound heights from the actual free-fall experiments, y_1 and y_2, into Equations (8) and (9) yielded the coefficient of restitution between Corydalis tuber and Q235 steel, x_1 = 0.728, and the coefficient of restitution between Corydalis tuber and soil, x_2 = 0.44. By setting x_1 and x_2 as the coefficients of restitution in the simulation experiments and repeating the trials 10 times, the average rebound height for Corydalis tuber and Q235 steel was 58.87 mm, and for Corydalis tuber and soil, it was 18.99 mm. The relative errors compared to the measured results from the actual experiments were 2.02% and 1.55%, respectively. This demonstrates that the calibrated simulation results were consistent with the experimental data. Ultimately, the coefficients of restitution for the discrete element simulation were determined to be 0.728 for Corydalis tuber and Q235 steel, and 0.44 for Corydalis tuber and soil.

Calibration of static friction coefficient

Based on the static friction angles of Corydalis tuber with Q235 steel and soil obtained from previous inclined plane tests (*Zhuang et al., 2023*), the established discrete element model of Corydalis tuber was utilized to create simulation experiments under actual test conditions, as shown in Figure 9.

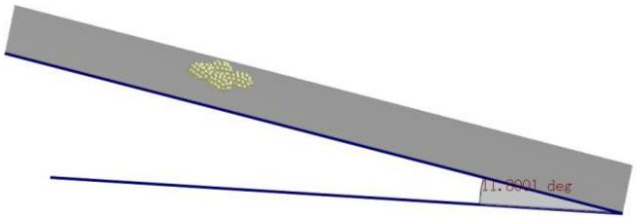

Fig. 9 - Ramp test simulation

In the simulation experiments, the coefficients of restitution between Corydalis tuber and Q235 steel, as well as soil, were predefined. The rolling friction coefficients and inter-particle parameters for Corydalis tuber were set to 0. Based on the actual experimental results, the static friction coefficient ranges for Corydalis tuber with Q235 steel and soil were selected as 0.1~0.7 and 0.3~0.9, respectively, with an increment of 0.1. The experimental results and the quadratic curve fitting results are shown in Figure 10.

The fitted equations for the static friction coefficient curve between Corydalis tuber and Q235 steel, as well as soil, are as follows:

$$y_3 = -20.714x_3^2 + 66.809x_3 + 2.3 \quad (10)$$

$$y_4 = -20.317x_4^2 + 65.666x_4 + 2.336 \quad (11)$$

in which:

y_3 – the inclination angle (Corydalis tuber and Q235 steel), [°];
x_3 – the static friction coefficient between Corydalis tuber and Q235 steel;
y_4 – the inclination angle (Corydalis tuber and soil), [°];
x_4 – the static friction coefficient between Corydalis tuber and soil.

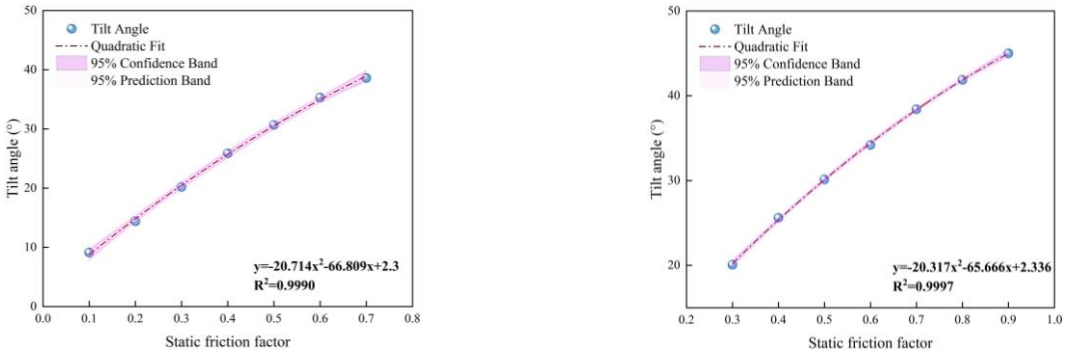

(a) Corydalis tuber - Q235 steel (b) Corydalis tuber - soil

Fig. 10 - The fitted curves of the static friction coefficient and inclination angle from simulation tests of Corydalis tuber with Q235 steel and soil

The coefficient of determination for regression equation y_3 was R^2 = 0.9990 with P = 0.0000009 << 0.05, and for y_4, it was R^2 = 0.9997 with P = 0.000000079 << 0.05, indicating that both models were highly significant. Substituting the average inclination angles from the actual inclined plane tests, y_3 = 40.52 and y_4 = 122.1, into Equations (10) and (11), yielded the static friction coefficients x_3 = 0.41 for Corydalis tuber with Q235 steel and x_4 = 0.76 for Corydalis tuber with soil. These static friction coefficients were then set as parameters for the simulation experiments, and 10 trials were conducted for each scenario. The resulting frictional inclination angle between Corydalis tuber and Q235 steel was 26.13°, with a relative error of 0.17% compared to the actual test. The frictional inclination angle between Corydalis tuber and soil was 40.46°, with a relative error of 0.41%. These results demonstrate that the calibrated simulation results closely aligned with the actual experimental data. Therefore, the static friction coefficients determined for the simulation experiments were finalized as 0.41 for Corydalis tuber with Q235 steel and 0.76 for Corydalis tuber with soil.

Calibration of rolling friction coefficient

Similarly, based on the rolling friction distances between Corydalis tuber and Q235 steel, as well as soil, measured in previous experiments, simulation experiments were constructed using the established discrete element model of Corydalis tuber under actual experimental conditions, as shown in Figure 11.

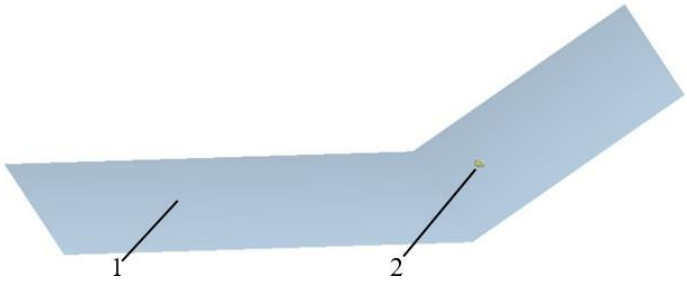

Fig. 11 - Rolling test simulation

1. Material plates; 2. Corydalis tuber.

In the simulation experiments, the coefficients of restitution and static friction coefficients between Corydalis tuber and Q235 steel, as well as soil, were predefined. The inter-particle contact parameters for Corydalis tuber were set to 0. The rolling friction coefficient range for Corydalis tuber and Q235 steel was selected as 0.01~0.07, and for Corydalis tuber and soil, it was 0.01~0.05, both with a step size of 0.01. The results of the simulation experiments and the fitted curves are shown in Figure 12.

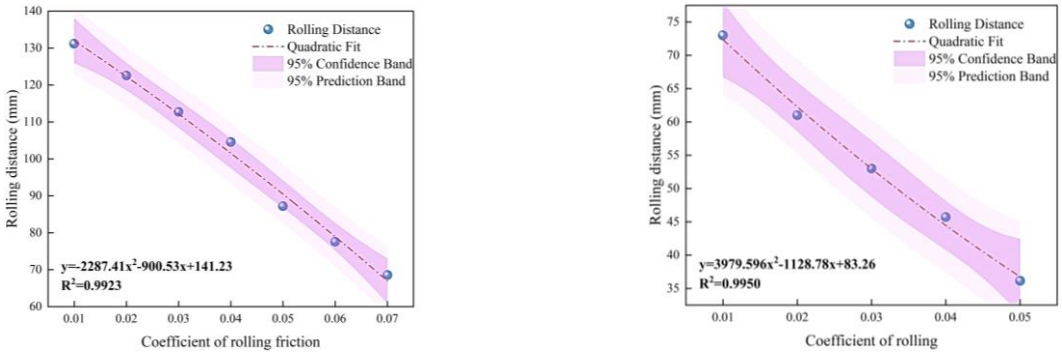

(a) Corydalis tuber - Q235 steel (b) Corydalis tuber - soil

Fig. 12 - The fitted curves of the rolling friction coefficient and rolling distance from simulation tests of Corydalis tuber with various Q235 steel and soil.

The fitted equations for the rolling friction coefficient curve between Corydalis tuber and Q235 steel, as well as soil, are as follows:

$$y_5 = -2287.41x_5^2 - 900.53x_5 + 141.23 \quad (12)$$

$$y_6 = 3979.59x_6^2 - 1128.78x_6 + 83.26 \quad (13)$$

in which: y_5 – the rolling distance (Corydalis tuber and Q235 steel), [m];
x_5 – the rolling friction coefficient between Corydalis tuber and Q235 steel;
y_6 – the rolling distance (Corydalis tuber and soil), [m];
x_6 – the rolling friction coefficient between Corydalis tuber and soil.

The coefficient of determination for regression equation y_5 was $R^2 = 0.9923$ with $P = 0.000058 \ll 0.05$, and for y_6, it was $R^2 = 0.9950$ with $P = 0.00495 \ll 0.05$, indicating that both models were highly significant. Substituting the average rolling distances from the actual rolling tests, $y_5 = 122.1$ mm and $y_6 = 49$ mm, into Equations (12) and (13), the rolling friction coefficients were calculated as $x_5 = 0.02$ for Corydalis tuber with Q235 steel and $x_6 = 0.03$ for Corydalis tuber with soil. These rolling friction coefficients were then set as parameters for the simulation experiments, and 10 trials were conducted for each scenario. The resulting rolling distance for Corydalis tuber with Q235 steel was 118.5 mm, with a relative error of 3.04% compared to the actual test. The rolling distance for Corydalis tuber with soil was 48.375 mm, with a relative error of 2.73%. These results demonstrate that the calibrated simulation results were generally consistent with the experimental data. Therefore, the rolling friction coefficients determined for the simulation experiments were finalized as 0.02 for Corydalis tuber with Q235 steel and 0.033 for Corydalis tuber with soil.

CONCLUSIONS

(1) Through experiments measuring the restitution coefficient, static friction coefficient, and rolling friction coefficient between Corydalis tuber and Q235 steel, as well as soil, the actual experimental values for these parameters were obtained. These tests included measurements of the restitution coefficient, static friction coefficient, and rolling friction coefficient for Corydalis tuber under both conditions.

(2) A three-dimensional contour model of Corydalis tuber was obtained using 3D scanning technology. The contour model obtained by scanning cannot be directly used in subsequent discrete element simulation experiments. In order to improve the accuracy of discrete element particle modeling of Corydalis tubers and the simulation accuracy, a multi-sphere bonded particle model of the Corydalis tuber was generated using the automatic filling method in the EDEM software.

(3) The simulation test takes the restitution coefficient, static friction coefficient and rolling friction coefficient between the Corydalis tuber and Q235 steel, and between the Corydalis tuber and soil as independent variables, and the collision height, friction angle and rolling distance as dependent variables. A second-order polynomial fitting was performed based on the simulation results, and the actual experimental values were substituted into the polynomial equation to obtain the simulated contact parameter values of the Corydalis tuber with Q235 steel and soil. The values were then verified based on the actual experimental measurements, and the relative error between the two was less than 5%.

REFERENCES

[1] Chen, Q., Chen, Y., Liu, Y., Huang, B., (2008). High yield cultivation techniques of Yuanhu. *Modern Agricultural Science and Technology*, vol.19, pp.71. (in Chinese), China;

[2] Chen, Z., Yu, J., Xue, D., Wang, Y., Zhang, Q., Ren, L., (2018). An approach to and validation of maize-seed-assembly modelling based on the discrete element method. *Powder Technology*, vol.328, pp.167-183. Switzerland. https://doi.org/10.1016/j.powtec.2017.12.007

[3] Chen, Z., Xue, D., Guan, W., Guo, J., Liu, Z., (2023). Performance Optimization of a Spoon Precision Seed Metering Device Based on a Maize Seed Assembly Model and Discrete Element Method. *Processes*, vol.11(11). pp.1-12. Switzerland. https://doi.org/10.3390/pr11113076

[4] Han, D., Zhang, D., Yang, L., Li, K., Zhang, T., Wang, Y., Cui, T., (2017). EDEM-CFD simulation and experiment of working performance of inside filling air-blowing seed metering device in maize. *Transactions of the Chinese Society of Agricultural Engineering*, vol.33(13), pp.23-31. (in Chinese) China. https://doi.org/10.11975/j.issn.1002-6819.2017.13.004

[5] He, K., Gao, J., Zhao, G., (2007). Advances in studies on chemistry, pharmacology, and quality control of Corydalis tuber. *Chinese Traditional and Herbal Drugs*, vol.12, pp.1909-1912. (in Chinese)

[6] Liu, W., He, J., Li, W., Li, X., Zheng, K., Wei, Z., (2018). Calibration of simulation parameters for potato minituber based on EDEM. *Transactions of the Chinese Society for Agricultural Machinery*, vol.49(5), pp.125-135. (in Chinese) China. https://doi.org/10.6041/j.issn.1000-1298.2018.05.014

[7] Ma, Z., Li, Y., Xu, L., (2013). Summarize of particle movements research in agricultural engineering realm. *Transactions of the Chinese Society for Agricultural Machinery*, vol.44(2), pp.22-29. (in Chinese). China. https://doi.org/10.6041/j.issn.1000-1298.2013.02.005

[8] Shi, L., Wu, J., Sun, W., Zhang, F., Sun, B., Liu, Q., Zhao, W., (2014). Simulation test for metering process of horizontal disc precision metering device based on discrete element method. *Transactions of the Chinese Society of Agricultural Engineering*, vol.30(8), pp.40-48. (in Chinese). China. https://doi.org/10.3969/j.issn.1002-6819.2014.08.005

[9] Sun, J., Liu, Q., Yang, F., Liu, Z., Wang, Z., (2022). Calibration of discrete element simulation paramet ers of sloping soil on loess plateau and its interaction with rotary tillage components. *Transactions of th e Chinese Society for Agricultural Machinery*, vol.53(1), pp.63-73. (in Chinese). China. https://doi.org/1 0.6041/j.issn.1000-1298.2022.01.007

[10] Sun, K., Yu, J., Liang, L., Wang, Y., Yan, D., Zhou, L., Yu, Y., (2022). A DEM-based general modelling method and experimental verification for wheat seeds. *Powder Technology*, Switzerland, vol.401(1173 53), pp.1-22. https://doi.org/10.1016/j.powtec.2022.117353

[11] Wang, H., Ding, K., Xia, J., Zhang, G., Wang, Y., Kang, Q., Tang, N., Liu, W., (2024). Calibration of Dis turbed-Saturated Paddy Soil Discrete Element Parameters Based on Slump Test. *Transactions of the Chinese Society for Agricultural Machinery*, vol.55(S2), pp.222–230. (in Chinese). China. https://doi.or g/10.6041/j.issn.1000-1298.2024.S2.022

[12] Xu, B., Zhang, Y., Cui, Q., Ye, S., Zhao, F., (2021). Construction of a discrete element model of buckwheat seeds and calibration of parameters. *INMATEH-Agricultural Engineering*, vol.64(2), pp.175-185. Romania. https://doi.org/10.356.33/inmateh-64-17

[13] Xu, B., Zheng, D., Cui, Q., (2022). Experimental research on three-level vibrating screening of buckwheat based on discrete element method. *INMATEH-Agricultural Engineering*, vol.68(3), pp.191-200. Romania. https://doi.org/10.35633/inmateh-68-19

[14] Xu, T., Yu, J., Yu, Y., Wang, Y., (2018). A modelling and verification approach for soybean seed particles using the discrete element method. *Advanced Powder Technology*, vol.29(12), pp.3274-3290. Japan. https://doi.org/10.1016/j.apt.2018.09.006

[15] Yang, S., Qiu, T., Ma, C., Li, X., Wang, L., & Liu, Y., (2023). Design and Test of Sugar Beet Combine Harvester Separation and Conveying Device. *Transactions of the Chinese Society for Agricultural Machinery*, vol.54(S1), pp.191–200. (in Chinese). China. https://doi.org/10.6041/j.issn.1000-1298.2023.S1.020

[16] Yu, Q., Liu, Y., Chen, X., Sun, K., Lai, Q., (2020). Calibration and experiment of simulation parameters for Panax notoginseng seeds based on DEM. *Transactions of the Chinese Society for Agricultural Machinery*, vol.51(2), pp.123-132. (in Chinese). China. https://doi.org/10.6041/j.issn.1000-1298.2020.02.014

[17] Zhang, Z., Zeng, C., Xing, Z., Xu, P., Guo, Q., Shi, R., Wang, Y., (2024). Discrete element modeling an d parameter calibration of safflower biomechanical properties. *International Journal of Agricultural and Biological Engineering*, vol.17(2), pp.37-46. China. https://doi.org/10.25165/j.ijabe.20241702.8857

[18] Zhao, P., Yu, T., Xu, G., Guo, R., Li, H., Xu, H., Jin, T., Ji, D., (2023). Design and drag reduction perfor mance analysis of a potato harvest shovel based on the surface texture characteristics of pangolin sca le. *INMATEH - Agricultural Engineering*, vol.70(2), pp.21–36. Romania. https://doi.org/10.35633/inmate h-70-02

[19] Zhao, J., Yu, J., Sun, K., Wang, Y., Liang, L., Sun, Y., Zhou, L., Yu, Y., (2024). A discrete element method model and experimental verification for wheat root systems. *Biosystems Engineering*, England, vol.244, pp.146-165. https://doi.org/10.1016/j.biosystemseng.2024.06.004

[20] Zhuang, H., Wang, X., Zhang, X., Cheng, X., Wei, Z., (2023). Discrete element-based design of key pa rameters for wheel rut tillage devices. *Engenharia Agrícola*, vol.43(3), pp.1-16. Brazil, http://dx.doi.org/10.1590/1809-4430-Eng.Agric.v43n3e20230039/2023